Terahertz studies of carrier dynamics and dielectric response of *n*-type, freestanding epitaxial GaN

W. Zhang, Abul K. Azad, and D. Grischkowsky[a)]
School of Electrical and Computer Engineering and Center for Laser and Photonics Research, Oklahoma State University, Stillwater, Oklahoma 74078

(Received 18 December 2002; accepted 28 February 2003)

We report the characterization of the complex conductivity and dielectric function of GaN by terahertz time-domain spectroscopy. Transmission measurements are performed on an *n*-type, 180-μm-thick, freestanding GaN crystal. Frequency dependent electron dynamics, power absorption and optical dispersion are observed over the frequency range from 0.1 to 4.0 THz. The measured conductivity is well fit by Drude theory. © *2003 American Institute of Physics.*
[DOI: 10.1063/1.1569988]

Epitaxial GaN has been recognized as an excellent candidate material for short wavelength light emission and high power electronic applications owing to the wide band gap (~3.4 eV), high breakdown field, large electron saturation velocity, and chemical stability at high temperatures. The optical and electrical properties of nitride materials have been studied extensively at ultraviolet (UV) to blue, and infrared frequency range using a variety of techniques including photoluminescence, magneto-optical infrared transmission, and infrared spectroscopic ellipsometry.[1–6] At UV frequencies, the Γ_5 and Γ_6 free excitons,[1] and longitudinal excitons[2] in GaN have been observed by emission measurements at low temperature (2 K). Using infrared ellipsometry, optical phonon modes over the frequency range from 300 to 1200 cm^{-1} in α-GaN have been determined at room temperature.[3] More interestingly, the multiquantum well based UV light emitting diode (LED) grown on a freestanding hydride-vapor-phase epitaxial GaN substrate showed more than a 1 order of magnitude increase in emission power at 340 nm compared with the LED grown on sapphire.[4] Recently, terahertz emission in nitride materials was observed with InGaN/GaN LED structures excited by the blue laser pulses from a frequency-doubled femtosecond Ti:sapphire laser.[7]

In this letter, we report the characterization of the complex electric conductivity and dielectric response of a GaN freestanding crystal over the frequency range from 0.1 to 4.0 THz using THz time-domain spectroscopy (TDS). The THz TDS technique has been widely used in characterization of various materials including molecular vapors,[8,9] semiconductors, [10–12] and conducting polymers.[13] According to the simple Drude model of conduction, the key parameters that determine the free carrier dynamics in a material are the plasma frequency ω_p and the carrier damping rate Γ. Since the values of $\omega_p/2\pi$ and $\Gamma/2\pi$ are THz frequencies, the measurements should be performed in this frequency range. To fit our transmission measurements through the GaN sample, the simple Drude model requires $\omega_p/2\pi = 1.82$ THz, and $\Gamma/2\pi = 0.81$ THz.

The GaN sample used in this study is an unintentionally doped, *n*-type, 5 mm×5 mm×180 μm thick, freestanding crystalline plate. Originally grown on *C*-plane sapphire by the hydride-vapor-phase epitaxy (HVPE) technique, the GaN layer was removed from the sapphire substrate by laser liftoff.[1,14] The *c* axis is perpendicular to the main planes of the sample. The sample is attached to a thin brass plate and centered over a 4-mm-diam hole in the plate, which defines the optical aperture. Another identical clear hole is used to take the reference signal designated as the input pulse. Our THz system for this measurement is a photoconductive switch based THz TDS spectrometer.[11] The system is aligned into a 4F confocal geometry that enables excellent beam coupling between the THz transmitter and receiver. In order to compress the THz beam to a diameter comparable to the size of the GaN sample while preserving the low frequency components, a pair of 25 mm focal length, high-resistivity, silicon lenses, separated by the confocal distance of 50 mm, are placed on the axis of THz beam between the two paraboloidal mirrors. As a result, midway between the two lenses, a frequency independent 2.8-mm-diam THz beam waist is obtained and on which the 4 mm sample clear aperture is centered.

The measured THz pulses transmitted through the sample and reference apertures are shown in Fig. 1(a). The peak amplitude of the first transmitted output pulse is about 30% that of the reference input pulse due to the frequency-dependent absorption and reflection of the GaN sample. The additional pulses are due to multiple reflections in the GaN sample. In order to increase the signal-to-noise ratio (S/N), each pulse curve is the average of ten individual measurements. The resulting background noise of the output pulse is at the level of 0.27 pA for which S/N=1100. The first signal pulse (multiplied by 3×) is compared in more detail to the reference pulse in Fig. 1(b) with an expanded time scale. Figure 1(c) shows the corresponding normalized amplitude spectra of the input pulse and output pulse train (multiplied by 3×). The oscillation in the output spectrum is due to the multiple reflections and is described by the well-known amplitude transmission function of a parallel dielectric slab.[15]

The complex spectrum of the transmitted pulse $E_0(\omega)$ is determined by the product of the input spectrum $E_i(\omega)$ and the total transmission function of the sample

a)Author to whom correspondence should be addressed; electronic mail: grischd@ceat.okstate.edu

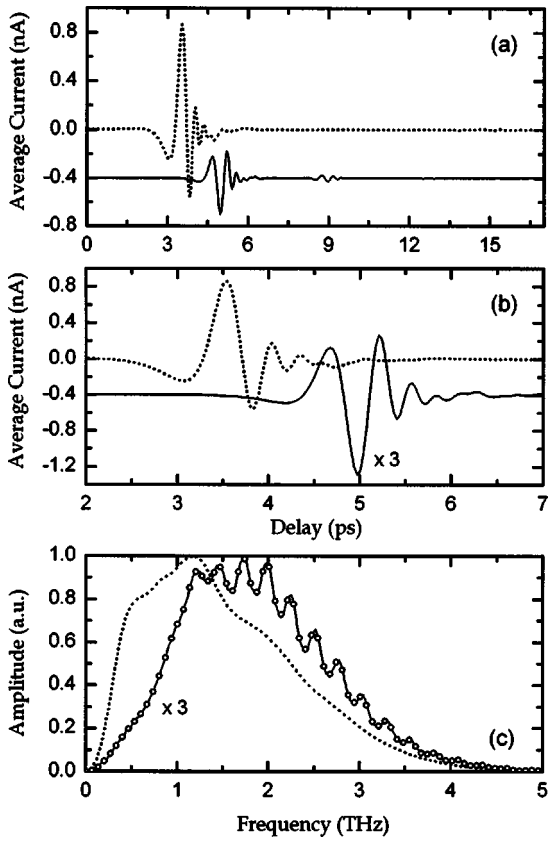

FIG. 1. (a) Measured reference THz pulse (dotted line) and output THz pulse with reflections (solid line offset by −0.4 nA); (b) measured reference THz pulse (dotted line) and the first output THz pulse (solid line offset by −0.4 nA and multiplied by 3×) with an expanded time scale; and (c) corresponding amplitude spectra of reference pulse (dotted line) and output pulse (solid line multiplied by 3×). The open circles give the output spectrum calculated from the reference spectrum using Eq. (1).

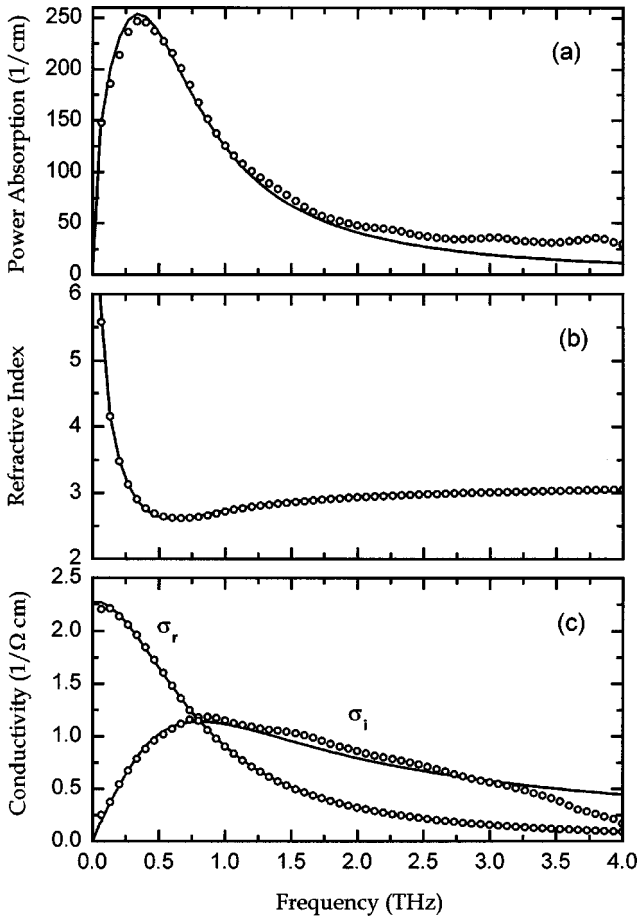

FIG. 2. Comparison of measured results (open circles) with Drude model fitting (solid lines): (a) power absorption coefficient α; (b) real part of refractive index n_r, and (c) complex electric conductivity σ_r and σ_i.

$$E_0(\omega)=E_i(\omega)\frac{t_{12}t_{21}\exp(ikL)\exp(-\alpha L/2)}{1+r_{12}r_{21}\exp(-\alpha L)\exp(i2kL)}, \qquad (1)$$

where $E_i(\omega)=E_R(\omega)\exp(-ik_0L)$; $E_R(\omega)$ is the reference spectrum, and the phase correction k_0L is due to the free-space occupied by the sample; t_{12}, t_{21} and r_{12}, r_{21} are the frequency-dependent complex Fresnel transmission and reflection coefficients, respectively; α is the power absorption coefficient, k is the sample wave vector $k=2\pi n/\lambda_0$, and L is the sample thickness. Because of the relatively clean separation in time between the main transmitted pulse and the first internal reflection, the initial data analysis was performed on the main pulse only. For this simpler case the denominator in Eq. (1) reduces to unity and the frequency spectrum of only the first transmitted pulse shows no oscillation. This approximation enabled the quite accurate determination of the power absorption α and index of refraction n of the sample, as shown in Figs. 2(a) and 2(b), respectively. Using these determined α and n, the full output pulse train was analyzed by Eq. (1) and very good agreement was obtained for both the spectral amplitude, as shown in Fig. 1(c), and phase of the entire output pulse train.

The frequency-dependent dielectric constant is defined as $\varepsilon=\varepsilon_d+i\sigma/(\omega\varepsilon_0)=(n_r+in_i)^2$; where ε_d is the complex contribution of the dielectric; σ is the complex conductivity; and n_r and n_i are the real and imaginary index of refraction, respectively. Using the relationship the real and imaginary conductivity shown in Fig. 2(c) were obtained from the experimentally determined α and n curves shown in Figs. 2(a) and 2(b).

The measured absorption, index of refraction, and complex conductivity were then theoretically fit using the simple Drude model[10,12] for which the complex conductivity is defined by $\sigma=i\varepsilon_0\omega_p^2/(\omega+i\Gamma)$. Three parameters were used to fit the experimental data: the plasma frequency $\omega_p/2\pi=1.82$ THz, the carrier damping rate $\Gamma/2\pi=0.81$ THz and the real part of the dielectric constant $\mathrm{Re}\,\varepsilon_d=9.4$. Given the reduced mass $m^*=0.22\,m_0$ for electrons in GaN,[5] these parameters correspond to a number density of $N=0.91\times10^{16}/\mathrm{cm}^3$ and a mobility $\mu=1570\ \mathrm{cm}^2/\mathrm{V\,s}$. According to Ref. 5, the free carriers in the HVPE GaN crystal are dominated by O donors over Si donors. In Fig. 2(a), the material absorption of intrinsic GaN, determined by the imaginary part of the dielectric constant $\mathrm{Im}\,\varepsilon_d$, is responsible for the difference between the Drude fitting curve and our measurement of power absorption at frequencies higher than 2 THz. The measured real part of refractive index n_r shown in Fig. 2(b) agrees quite well with Drude fitting. The real and imaginary electric conductivity calculated from the optical data are shown in Fig. 2(c), respectively, where Drude fitting agrees well with the measurements.

For the data shown in Fig. 1 the receiver antenna had a total length of 10 μm. In order to measure the sample with more precision below 1 THz, the receiver antenna was re-

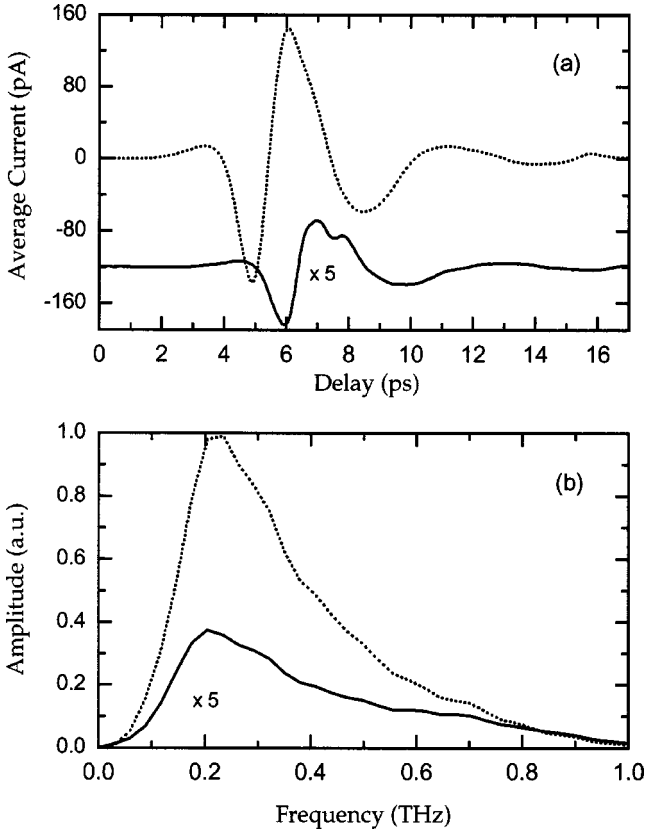

FIG. 3. (a) Measured reference THz pulse (dotted line) and output THz pulse (solid line offset by −120 pA and multiplied by 5×) and (b) corresponding amplitude spectra of reference pulse (dotted line) and output pulse (solid line multiplied by 5×).

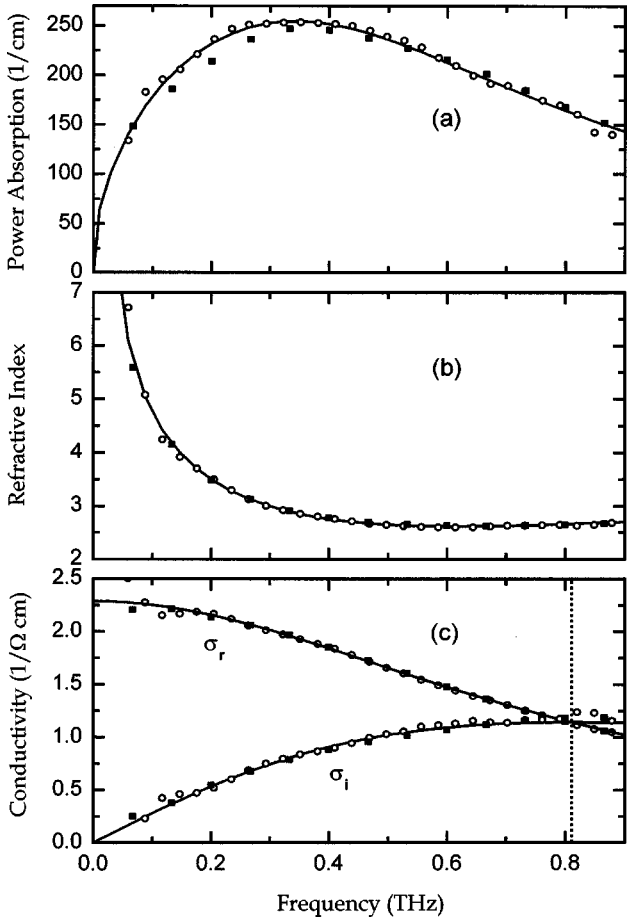

FIG. 4. Comparison of measured results (open circles) low-frequency receiver with Drude model fitting (solid lines): (a) power absorption coefficient α; (b) real part of refractive index n_r; and (c) complex electric conductivity σ_r and σ_i. The dotted vertical line gives $\Gamma/2\pi = 0.81$ THz. The solid squares are the experimental results from Fig. 2.

placed by one with a total length of 100 μm. Figure 3 shows the resulting measured transmitted pulses with this 100 μm antenna and the corresponding amplitude spectra. Due to the strong absorption at this lower frequency range, the amplitude of the transmitted output pulse is more than 1 order of magnitude smaller than the reference input pulse, and the reflected pulses were not observed. Using the same data analysis, the measured power absorption, refractive index, and complex conductivity are shown in Fig. 4 as the open circles. It should be noted that for Drude theory, the real and imaginary conductivity curves intersect at the carrier damping rate $\Gamma/2\pi$. This feature is shown in Figs. 2(c) and 4(c) for both our analysis and observations. Consequently, our high quality data enabled $\Gamma/2\pi = 0.81$ THz to be directly determined by the measurements, shown in Fig. 4(c). Using the same $\omega_p/2\pi = 1.82$ THz, $\Gamma/2\pi = 0.81$ THz, and $\mathrm{Re}\,\varepsilon_d = 9.4$ as that in Fig. 2, the same Drude fitting shows excellent agreement with the measurements, and verifies accuracy of the broadband results presented in Fig. 2, which are indicated in Fig. 4 by the solid squares.

The authors acknowledge D. C. Reynolds, D. C. Look for stimulating discussions and support, and the Wood-Witt GaN program at Wright State University for providing the GaN crystal. The authors also thank S. S. Park of Samsung, who grew the crystal. This work was partially supported by the National Science Foundation and the Army Research Office.

[1] D. C. Reynolds, D. C. Look, B. Jogai, A. W. Saxler, S. S. Park, and J. Y. Hahn, Appl. Phys. Lett. **77**, 1879 (2000).
[2] D. C. Reynolds, B. Jogai, and T. C. Collins, Appl. Phys. Lett. **80**, 3928 (2002).
[3] A. Kasic, M. Schubert, S. Einfeldt, D. Hommel, and T. E. Tiwald, Phys. Rev. B **62**, 7365 (2000).
[4] A. Yasan, R. McClintock, K. Mayes, S. R. Darvish, H. Zhang, P. Kung, M. Razeghi, S. K. Lee, and J. Y. Han, Appl. Phys. Lett. **81**, 2151 (2002).
[5] W. J. Moore, J. A. Freitas, Jr., S. K. Lee, S. S. Park, and J. Y. Han, Phys. Rev. B **65**, 081201 (2002).
[6] D. D. Chen, M. Smith, J. Y. Lin, H. X. Jiang, S. H. Wei, M. A. Khan, and C. J. Sun, Appl. Phys. Lett. **68**, 2784 (1996).
[7] J. Y. Sohn, J. S. Yahng, D. J. Park, E. Oh, D. S. Kim, G. D. Sanders, C. J. Stanton, and D. S. Citrin, Proceedings of QELS' 2002, Long Beach, CA, May 19–24, 2002, paper QThC5.
[8] M. van Exter, Ch. Fattinger, and D. Grischkowsky, Opt. Lett. **14**, 1128 (1989).
[9] H. Harde, R. A. Cheville, and D. Grischkowsky, J. Phys. Chem. A **101**, 3646 (1997).
[10] M. van Exter and D. Grischkowsky, Phys. Rev. B **41**, 12140 (1990).
[11] D. Grischkowsky, S. Keiding, M. van Exter, and Ch. Fattinger, J. Opt. Soc. Am. B **7**, 2006 (1990).
[12] T. I. Jeon and D. Grischkowsky, Phys. Rev. Lett. **78**, 1106 (1997).
[13] T. I. Jeon, D. Grischkowsky, A. K. Mukherjee, and R. Menon, Appl. Phys. Lett. **77**, 2452 (2000).
[14] M. K. Kelly, R. P. Vaudo, V. M. Phanse, L. Görgens, O. Ambacher, and M. Stutzmann, Jpn. J. Appl. Phys., Part 2 **38**, L217 (1999).
[15] M. Born and E. Wolf, *Principles of Optics*, 7th (expanded) ed. (Cambridge University Press, Cambridge, UK, 2002), p. 65, Eq. (58).